Demography and dispersal at a grass-shrub ecotone: a spatial integral projection model for woody plant encroachment

Trevor Drees[a], Brad M. Ochocki[b], Scott L. Collins[c], and Tom E.X. Miller[*][b]

[a]Department of Biology, Penn State University, State College, PA USA

[b]Program in Ecology and Evolutionary Biology, Department of BioSciences, Rice University, Houston, TX USA

[c]Department of Biology, University of New Mexico, Albuquerque, NM USA

March 23, 2023

* Corresponding author: tom.miller@rice.edu

Abstract

The encroachment of woody plants into grasslands is a global phenomenon with implications for biodiversity and ecosystem function. Understanding and predicting the pace of expansion and the underlying processes that control it are key challenges in the study and management of woody encroachment. Theory from spatial population biology predicts that the occurrence and speed of population expansion should depend sensitively on the nature of conspecific density dependence. If fitness is maximized at the low-density encroachment edge then shrub expansion should be "pulled" forward. However, encroaching shrubs have been shown to exhibit positive feedbacks, whereby shrub establishment modifies the environment in ways that facilitate further shrub recruitment and survival. In this case there may be a fitness cost to shrubs at low density causing expansion to be "pushed" from behind the leading edge. We studied the spatial dynamics of creosotebush (*Larrea tridentata*), which has a history of encroachment into Chihuahuan Desert grasslands over the past century. We used demographic data from observational censuses and seedling transplant experiments to test the strength and direction of density dependence in shrub fitness along a gradient of shrub density at the grass-shrub ecotone. We also used seed-drop experiments and wind data to construct a mechanistic seed dispersal kernel, then connected demography and dispersal data within a spatial integral projection model (SIPM) to predict the dynamics of shrub expansion. The SIPM predicted that, contrary to expectations based on potential for positive feedbacks, the shrub encroachment wave is "pulled" by maximum fitness at the low-density front. However, the predicted pace of expansion was strikingly slow (ca. 8 cm/yr), and this prediction was supported by independent re-surveys of the ecotone showing little to no change in spatial extent of shrub cover over 12 years. Encroachment

2

speed was acutely sensitive to seedling recruitment, suggesting that this population may be primed for pulses of expansion under conditions that are favorable for recruitment. Our integration of observations, experiments, and modeling reveals not only that this ecotone is effectively stalled under current conditions, but also *why* that is so and how that may change as the environment changes.

Keywords

density-dependence, ecotones, woody encroachment, shrubs, integral projection model, dispersal, Allee effects

3

Introduction

The recent and ongoing encroachment of shrubs and other woody plants into adjacent grasslands has caused significant vegetation changes across arid and semi-arid landscapes worldwide (Cabral et al., 2003; Gibbens et al., 2005; Goslee et al., 2003; Parizek et al., 2002; Roques et al., 2001; Trollope et al., 1989; Van Auken, 2009, 2000). The process of encroachment generally involves increases in the number or density of woody plants in both time and space (Van Auken, 2000), which can drive shifts in plant community structure and alter ecosystem processes (Knapp et al., 2008; Ravi et al., 2009; Schlesinger and Pilmanis, 1998; Schlesinger et al., 1990). Other effects of encroachment include changes in ecosystem services (Kelleway et al., 2017; Reed et al., 2015), declines in biodiversity (Brandt et al., 2013; Ratajczak et al., 2012; Sirami and Monadjem, 2012), and economic losses in areas where the proliferation of shrubs adversely affects grazing land and pastoral production (Morford et al., 2022).

Woody plant encroachment can be studied through the lens of spatial population biology as a wave of individuals that may expand across space and over time (Kot et al., 1996; Neubert and Caswell, 2000; Pan and Lin, 2012; Wang et al., 2002). Theory predicts that whether the wave can advance and the speed at which it does so depends on two processes: local demography and dispersal of propagules. First, local demographic processes include recruitment, survival, growth, and reproduction, which collectively determine the rate at which newly colonized locations increase in density and produce new propagules. Second, colonization events are driven by the spatial dispersal of propagules, which is commonly summarized as a probability distribution of dispersal distances, or "dispersal kernel". Expansion speed is highly dependent upon the shape of the dispersal kernel and can be strongly influenced by long-distance dispersal events in the tail

4

of the distribution (Skarpaas and Shea, 2007). Both demography and dispersal may depend on plant size, since larger plants often have improved demographic performance and release seeds from greater heights, leading to longer dispersal distances (Nathan et al., 2011). Accounting for population structure, including size structure, may therefore be important for understanding and predicting encroachment dynamics (Neubert and Caswell, 2000).

Theory predicts that the nature of conspecific density dependence is another critical feature of expansion dynamics but this is rarely studied in the context of woody plant encroachment. Expansion waves typically correspond to gradients of conspecific density – high in the back and low at the front – and demographic rates may be sensitive to density due to intraspecific interactions like competition or facilitation. If the demographic effects of density are strictly negative due to competitive effects that increase with density, then demographic performance is expected to be maximized as density goes to zero at the leading edge of the wave. Under these conditions, the wave is "pulled" forward by individuals at the low-density vanguard (Kot et al., 1996), and targeting these individuals and locations would be the most effective way to slow down or prevent encroachment. However, woody encroachment often involves positive feedbacks whereby shrub establishment modifies the environment in ways that facilitate further shrub recruitment. For example, woody plants can modify their micro-climates in ways that elevate nighttime minimum temperatures, promoting conspecific recruitment and survival for freeze-sensitive species (D'odorico et al., 2013; Huang et al., 2020). Positive density dependence (or Allee effects) causes demographic rates to be maximized at higher densities behind the leading edge, which "push" the expansion forward, leading to qualitatively different expansion dynamics (Kot et al., 1996; Lewis and Kareiva, 1993; Sullivan et al., 2017; Taylor and Hastings, 2005; Veit and Lewis, 1996). Pushed expan-

5

sion waves generally have different shapes (steeper density gradients) and slower speeds than pulled waves (Gandhi et al., 2016), and may require different strategies for managing or decelerating expansion (Taylor and Hastings, 2005). Under some conditions, pushed waves may fail entirely, "pinning" population boundaries in place (Keitt et al., 2001). The potential for positive feedbacks is well documented in woody encroachment systems as a key feature of bi-stability (the existence of woody and herbaceous habitats as alternative stable states: Wilcox et al. (2018)) but it remains unclear whether and how strongly these feedbacks decelerate shrub expansion or prevent it altogether.

In this study, we linked shrub dynamics at grass-shrub ecotones to ecological theory for spreading populations, with the goals of understanding the spatial dynamics that emerge from seed dispersal and density-dependent demography at the edge of the encroachment wave, and determining whether the wave is pushed or pulled. Throughout the aridlands of the southwestern United States, shrub encroachment into grasslands is well documented (D'Odorico et al., 2012) but little is known about the dispersal and demographic processes that govern it. Our work focused on creosotebush (*Larrea tridentata*) in the northern Chihuahuan Desert. This native shrub has encroached into grasslands over the past 150 years, leading to decreased cover of black grama grass (*Bouteloua eriopoda*), the dominant foundation species of Chihuahuan desert grassland (Buffington and Herbel, 1965; Gardner, 1951; Gibbens et al., 2005). As in many woody encroachment systems, creosotebush expansion generates ecotones marking a transition from dense shrubland to open grassland, with a transition zone in between where shrubs can often be found interspersed among grasses (Fig. 1).

Historically, creosotebush encroachment into grasslands is believed to have been driven by a combination of factors including overgrazing, drought, variability in rainfall, and suppression of fire regimes (Moreno-de las Heras et al., 2016). These shrubs

are also thought to further facilitate their own encroachment through positive feedbacks (D'Odorico et al., 2012; Grover and Musick, 1990) by modifying their environment in ways that favor survival, growth, and recruitment, including changes to the local micro-climate (D'Odorico et al., 2010) and rates of soil erosion (Turnbull et al., 2010). Such positive feedbacks also involve suppression of herbaceous competitors, reducing competition as well as the amount of flammable biomass used to fuel the fires that keep creosotebush growth in check (Van Auken, 2000).

Our work was conducted at the Sevilleta Long-Term Ecological Research (LTER) site in central New Mexico, where the most recent major advance of creosotebush into desert grassland is estimated to have occurred in the 1950s (Moreno-de las Heras et al., 2016). More recently, the shrub encroachment wave has exhibited little apparent advance. For example, between 2001 and 2013, we saw very little change in the spatial extent of shrub cover measured along two permanent transects (Fig. 2), small enough to be conservatively attributable to measurement error. We therefore sought to mechanistically understand whether this shrub encroachment wave is indeed stalled under current conditions, why that is so, and whether it is poised to remain that way. One hypothesis is that the positive feedbacks that favor bi-stability – maintaining shrubland as shrubland and grassland as grassland – may inhibit advance of the encroachment wave. This hypothesis predicts fitness penalties for shrubs at the low-density vanguard (pushed-wave dynamics). Alternatively, positive feedbacks may be absent or insufficient to prevent shrub encroachment of grassland, but the pace of encroachment may be limited by other factors. This hypothesis predicts that the encroachment wave is pulled forward (fitness maximized at low density) but may be pulled very slowly or episodically due to constraints associated with short seed dispersal and low seedling recruitment (Boyd and Brum, 1983; Moreno-de las Heras et al., 2016). Our study was designed to differentiate

7

We used a combination of observational and experimental data from grass-shrub ecotones in central New Mexico to parameterize a spatial integral projection model (SIPM) that predicts the speed of encroachment (m/yr) resulting from lower-level demographic and dispersal processes. Our data came from demographic surveys and experimental transplants along replicate ecotone transects spanning a gradient of shrub density, and from seed drop experiments to estimate the properties of the dispersal kernel. We focused on wind dispersal of seeds, since little is known about the natural history of dispersal in this system and the seeds lack adaptations to attract frugivorous animals, such as bright coloration or fleshy fruit, though they may be moved by granivores. We built mechanistic dispersal kernels that predict seed movement based on properties of maternal plants, seeds, and wind; because it does not account for secondary dispersal vectors, this approach provided a conservative first step toward understanding seed movement. The SIPM accounts for size-structured demography of creosotebush, allows us to test whether shrub expansion is pulled by the low-density front or pushed from the high-density core, and identifies the local (demographic) and spatial (seed dispersal) life cycle transitions that most strongly limit encroachment. We address the following specific questions:

1. What are the strength and direction of density dependence in demographic vital rates along shrub encroachment ecotones?

2. What is the seed dispersal kernel and how does it vary with maternal plant size?

3. What is the predicted rate of expansion and which lower-level processes most strongly affect the expansion speed?

8

Materials and methods

Study species

Creosotebush (*Larrea tridentata*) is a perennial, drought-resistant shrub that is native to the arid and semiarid regions of the southwestern United States and northern Mexico. High-density areas of creosotebush consist largely of barren soil between plants due to the "islands of fertility" these shrubs create around themselves (Reynolds et al., 1999; Schlesinger et al., 1996), though lower-density areas will often contain grasses in the inter-shrub spaces (Fig. 1). Elsewhere in North America creosotebush can produce clonal rings though asexual reproduction (Vasek, 1980) but this does not occur in our northern Chihuahuan desert study region, where creosotebush genetic diversity is high (Duran et al., 2005). The small yellow flowers of creosotebush give rise to pubescent spherical fruits several *mm* in diameter; these fruits consist of five carpels, each of which contains a single seed. Seeds are dispersed from the parent plant by gravity and wind, with the possibility for seeds to subsequently be transported by animals or water (Maddox and Carlquist, 1985). The foliage is dark green, resinous, and unpalatable to most grazing and browsing animals (Mabry et al., 1978).

Study site

We conducted our work at the Sevilleta National Wildlife Refuge (SNWR), a Long-Term Ecological Research (SEV-LTER) site in central New Mexico. The refuge exists at the intersection of several eco-regions, including the northern Chihuahuan Desert, Great Plains grassland, and steppes of the Colorado Plateau. Annual precipitation is approximately 250*mm*, with the majority falling during the summer monsoon from June to September.

9

The recruitment events that facilitate creosotebush expansion are thought to be episodic (Peters and Yao, 2012), and this may be linked to fluctuations in monsoon precipitation (Bowers et al., 2004; Boyd and Brum, 1983). SNWR has been closed to cattle grazing since 1973. Wildfires at SNWR are allowed to burn but there have been no major fires near the grass-shrub ecotone since 2003. Our study years included one unusually wet and one unusually dry monsoon season (Appendix S2, Fig. S1A).

Demographic data

Ecotone transects

We collected demographic data during early June of every year from 2013-2017. This work was conducted at four sites in the eastern part of SNWR (one site was initiated in 2013 and the other three in 2014), with three transects at each site. All transects were situated along a shrubland-grassland ecotone so that a full range of shrub densities was captured: each transect spanned core shrub areas, grassland with no or few shrubs, and the transition between them. Lengths of these transects varied from 200 to 600 m and were determined by the strength of vegetation transition since "steep" transitions required less length to capture the full range of shrub density.

We quantified shrub density in 5-meter "windows" along each transect, including all shrubs within one meter of the transect on either side (shrubs that partially overlapped with the census area were included). Densities were quantified once for each transect (in 2013 or 2014) and were assumed to remain constant for the duration of the study, a reasonable assumption for a species with very low recruitment and very high survival of established plants (see Results). Given the population's size structure, we weighted the density of each window by the sizes of the plants, which we quantified as volume (cm^3). Volume was calculated as that of an elliptic cone (McAuliffe et al., 2007): $V_i = \frac{\pi h}{3} \frac{lw}{4}$

10

where l, w, and h are the maximum length, maximum width, and height, respectively. Maximum length and width were measured so that they were always perpendicular to each other, and height was measured from the base of the woody stem at the soil surface to the tallest part of the shrub. The weighted density for a window was then expressed as log(volume) summed over all plants in the window.

Observational census

At approximately 50-m intervals along each transect we tagged up to 10 plants for annual demographic census and recorded their local (5-m resolution) window so that we could connect individual demographic performance to local density. These tagged shrubs were revisited every June and censused for survival (alive/dead), size (width, length, and height, as above), flowering status, and fertility of flowering plants (numbers of flower-buds, flowers, and fruits). In instances where shrubs had large numbers of reproductive structures that would be difficult to reliably count (a large shrub may have thousands of flowers or fruits), we made counts on a fraction of the shrub and extrapolated to esti-mate whole-plant reproduction. Creosotebush does not have one discrete reproductive event per year; instead, flowering may occur throughout much of the warm season. By combining counts of buds, flowers, and fruits we intended to capture a majority of the season's reproductive output, assuming that all buds and flowers will eventually become fruits. Our measurements of reproductive output are therefore conservative and may un-derestimate total seed production for an entire transition year. Each year, we searched for new recruits within $1m$ on either side of the transect. New recruits were tagged and added to the demographic census. The observational census included a total of 522 unique individuals.

11

Transplant experiment

We conducted a transplant experiment in 2015 to test how shrub density affects seedling survival. This approach complemented observational estimates of density dependence and filled in gaps for a part of the shrub life cycle that was rarely observed due to low recruitment. Seeds for the experiment were collected from plants in our study population in 2014. Seeds were germinated on Pro-Mix potting soil (Quakertown, PA) in Fall 2014 and seedlings were transferred to 3.8 cm-by-12.7 cm cylindrical containers and maintained in a greenhouse at Rice University. Seedlings were transported to SNWR and transplanted into the experiment during July 27-31, 2015. Transplant timing was intended to coincide with the monsoon season, when most natural recruitment occurs.

The transplant experiment was conducted at the same four sites and three transects per site as the observational demographic census, where we knew weighted shrub densities at 5-m window resolution. We established 12 1-m by 1-m plots along each transect and these were intentionally placed to capture density variation: four plots were in windows with zero shrubs, four plots were placed in the top four highest-density windows on the transect, and the remaining four plots were randomly distributed among the remaining windows with weighted density greater than zero. Plots were placed in the middle of each 5-m window (at meter 2.5) and were divided into four 0.5-m by 0.5-m subplots. We divided each subplot into nine squares (0.125-m by 0.125-m) and recorded ground cover of each square as one of the following categories: bare ground, creosote-bush, black grama (*B. eriopoda*), blue grama (*B. gracilis*), other grass, or "other". Each subplot received one transplanted shrub seedling, for a total of 48 transplants per transect, 144 transplants per site, and 576 transplants in the entire experiment. Each site was set up on a different day and there was a significant monsoon event between setup of the third and fourth sites. This resulted in differential mortality that appears to be related

12

to site (captured as a statistical random effect) but more likely reflects the timing of the monsoon event relative to planting (moist soil likely promoted transplant survival). We revisited the transplant experiment on October 24, 2015 to survey mortality. After that first visit, transplants were censused along with the naturally occurring plants each June, following the methods described above.

Demographic analysis

We fit statistical models to the demographic data and used AIC-based model selection to evaluate empirical support for alternative candidate models. The top statistical models were then used as the vital rate sub-models of the SIPM, so there is a strong connection between the statistical and population modeling, as is typical of integral projection modeling. Our analyses focused on the following demographic vital rates: survival, growth, probability of flowering, fertility (flower and fruit production), seedling recruitment, and seedling size. Most of these vital rates were modeled as a function of plant size, and all of them included the possibility of density dependence.

The alternative hypotheses of pushed versus pulled wave expansion rest on how the rate of population increase (λ), derived from the combination of all vital rates, respond to density. We were particularly interested in whether demographic performance was maximized as local density goes to zero (pulled) or at non-zero densities behind the wave front (pushed). To flexibly model density dependence and detect non-monotonic responses, we used generalized additive models in the R package 'mgcv' (Wood, 2017). For each vital rate, we fit candidate models with or without a smooth term for local weighted density, among other possible covariates. To avoid over-fitting, we set the 'gamma' argument of gam() to 1.8, which increases the complexity penalty, results in smoother fits (Wood, 2017), and makes our approach more conservative (other gamma

values yielded qualitatively similar results). We pooled data across transition years for analysis. All models included the random effect of transect (12 transects across 4 sites); we did not attempt to model both site and transect-within-site random effects due to the low numbers of each. All vital rate functions used the natural logarithm of volume (cm^3) as the size variable and the sum of log(volume) as the weighted density of a transect window.

Survival. We modeled survival (alive or dead) in year $t + 1$ as a Bernoulli random variable with three candidate models for survival probability. These included smooth terms for initial size in year t only (1), initial size and weighted density (2), and both smooth terms plus an interaction between initial size and weighted density (3). We analyzed survival of experimental transplants and observational census plants together in the same analyses, with a fixed effect of transplant status (yes/no) included in all candidate models. Since recruits and thus mortality events were both very rare in the observational survey, this approach allowed us to "borrow strength" over both data sets to generate a predictive function for size- and possibly density-dependent survival while statistically accounting for differences between experimental and naturally occurring plants. Because we had additional, finer-grained cover data for the transplant experiment that we did not have for the observational census, we conducted an additional stand-alone analysis of transplant survival that explored the influence of shrub and grass density at multiple spatial scales (Appendix S3).

Growth. We modeled size in year $t + 1$ (a continuous variable) as a Gaussian random variable, with nine candidate models for growth. The simplest model (1) defined the mean of size in year $t + 1$ as a smooth function of size in year t and constant variance. Models (2) and (3) had constant variance but the mean included smooth terms for initial

14

size and weighted density (2) or both smooth terms plus an interaction between initial size and weighted density (3). Models 4-6 had the same mean structure as 1-3 but defined the standard deviation of size in year $t + 1$ as a smooth function of initial size. Models 7-9 mirrored 4-6 and additionally included a smooth term for weighted density in the standard deviation. Modeling growth correctly is important because it defines the probability of any future size conditional on current size, a critical element of the IPM transition kernel. We verified that the AIC-selected model described the data well by simulating data from it and comparing the moments (mean, variance, skewness, and kurtosis) of simulated and real data.

Flowering and fruit production. We modeled shrub reproductive status (vegetative or flowering) in year t as a Bernoulli random variable with three candidate models for flowering probability. These included smooth terms for current size (in year t) only (1), size and weighted density (3), and both smooth terms plus an interaction between size and weighted density. We modeled the reproductive output of flowering plants (the sum of flowerbuds, open flowers, and fruits) in year t as a negative binomial random variable. There were three candidate models for mean reproductive output that corresponded to the same three candidates for flowering probability.

Recruitment and recruit size. We modeled seedling recruitment in each transect window as a binomial random variable given the number of seeds (successes) and the total seeds produced in that window in the preceding year (trials). There were two candidate models, with and without an influence of weighted density on the per-seed recruitment probability. To estimate window-level seed production, we used the best-fit models for flowering and fruit production and applied this to all plants in each window that we observed in our initial density surveys. We assume that recruits come from the previous

year's seeds and not from a long-lived soil seed bank. This assumption might lead us to over-estimate the recruitment rate, since existence of a seed bank would inflate the denominator of seedlings-per-seed. However, a previous study at SNWR found relatively low densities of viable creosotebush seeds in soil, suggesting that this species does not form a persistent seed bank (Moreno-de las Heras et al., 2016). Our estimation of recruitment combines the processes of seed germination and early seedling survival preceding the census.

We modeled recruit size (a continuous variable) as a Gaussian-distributed random variable and fit four candidate models including an influence of weighted density on mean, variance, both, and neither.

Density-dependent IPM

The size- and density-dependent statistical models comprised the sub-models of a density dependent Integral Projection Model (IPM) that we used to evaluate how the shrub population growth rate responded to conspecific density; we present this non-spatial model before layering on the spatial dynamics generated by seed dispersal. A basic density-independent IPM predicts the number of individuals of size x' at time $t+1$ ($n(x', t+1)$) based on a demographic projection kernel (K_{dem}) that gives the rates of transition from sizes x to x' from times t to $t+1$ and is integrated over the size distribution from the minimum (x_{min}) to maximum (x_{max}) sizes. In a density-dependent IPM, components of the projection kernel may respond to population abundance and structure:

$$n(x', t+1) = \int_{x_{min}}^{x_{max}} K_{dem}(x', x, \tilde{n}(t)) n(x, t) \, dx \qquad (1)$$

Here, $\tilde{n}(t)$ is some function of population structure $n(x,t)$ such as the total density of conspecifics ($\tilde{n}(t) = \int n(x,t) \, dx$) or, as in our case, total density weighted by size ($\tilde{n}(t) =$

16

$\int xn(x, t) dx$). For simplicity, in the analyses that follow we do not model density as a dynamic state variable; instead, we treat density as a static covariate ($\tilde{n}(t) = \tilde{n}$) and evaluate the IPM at a range of density values. As in our statistical modeling, the size variable of the IPM (x, x') was $log(cm^3)$.

For our model, the size- and density-dependent demographic transitions captured by the projection kernel include growth or shrinkage (g) from size x to $x\prime$ conditioned on survival (s) at size x (combined growth-survival function $G(x\prime, x, \tilde{n}) = g(x\prime, x, \tilde{n})s(x, \tilde{n})$), and the production of new size-$x\prime$ individuals from size-x parents ($Q(x\prime, x, \tilde{n})$). Reproduction reflects the probability of flowering at size x (p), the number of seeds produced by flowering plants (d), the per-seed probability of recruitment (m), and the size distribution of recruits (c). Collectively, the rate at which x-sized individuals produce $x\prime$-sized individuals at density $\tilde{n}$ is given by the combined reproduction-recruitment function $Q(x\prime, x, \tilde{n}) = p(x, \tilde{n})d(x, \tilde{n})m(\tilde{n})c(x\prime, \tilde{n})$. Thus, we can express the projection kernel as:

$$K_{dem}(x', x, \tilde{n}) = G(x', x, \tilde{n}) + Q(x', x, \tilde{n}) \tag{2}$$

For analysis, we evaluated the IPM kernel over a range of local densities from the minimum to the maximum of weighted density values observed in the 5-meter windows ($0 \leq \tilde{n} \leq \tilde{n}_{max}$). At each density level, we discretized the IPM kernel into a 200×200 matrix and calculated the asymptotic growth rate $\lambda(\tilde{n})$ as its leading eignevalue. We extended the lower (x_{min}) and upper (x_{max}) integration limits to avoid unintentional "eviction" using the floor-and-ceiling method (Williams et al., 2012).

We sought to characterize the shape of density dependence – whether fitness declined monotonically or not with increasing density – and quantified uncertainty in the density-dependent growth rate $\lambda(\tilde{n})$ by bootstrapping our data. For each bootstrap, we randomly sampled 75% of our demographic data, re-ran the statistical modeling and

17

368 model selection, and used the top vital rate models to generate $\lambda(\tilde{n})$ for that data subset.

369 We repeated this procedure for 500 bootstrap replicates.

370 ## *Dispersal modelling*

371 *WALD dispersal model.* Dispersal kernels were calculated using the WALD, or Wald ana-

372 lytical long-distance dispersal, model that uses a mechanistic approach to predict disper-

373 sal patterns of plant propagules by wind. The WALD model, which is based in fluid dy-

374 namics, can serve as a good approximation of empirically-determined dispersal kernels

375 (Katul et al., 2005; Skarpaas and Shea, 2007) and may be used when direct observations

376 of dispersal are not available. Under the assumptions that wind turbulence is low, wind

377 flow is vertically homogenous, and terminal velocity is achieved immediately upon seed

378 release, the WALD model simplifies a Lagrangian stochastic model to create a dispersal

379 kernel that estimates the likelihood a propagule will travel a given distance (Katul et al.,

380 2005). Our dispersal kernel takes the form of the inverse Gaussian distribution, using r

381 to denote dispersal distance:

382
$$p(r) = \left(\frac{\lambda'}{2\pi r^3} \right)^{\frac{1}{2}} \exp \left[-\frac{\lambda'(r - \mu')^2}{2\mu'^2 r} \right] \tag{3}$$

383 Here, λ' is the location parameter and μ' is the scale parameter, which depend on

384 environmental and plant-specific properties of the study system. (We use λ' for consis-

385 tency with notation in related papers, but λ' the dispersal location parameter should not

386 be confused with λ the geometric growth rate.) The location and scale parameters are

387 defined as $\lambda' = (H/\sigma)^2$ and $\mu' = HU/F$; these are functions of the height H of seed

388 release, wind speed U at seed release height, seed terminal velocity F, and the turbulent

389 flow parameter σ that depends on both wind speed and local vegetation roughness. We

390 parameterized the WALD dispersal kernel using windspeed data from the SEV-LTER

18

weather station nearest our study site (Moore and Hall, 2022) and seed terminal velocity data from laboratory-based seed-drop experiments (Appendix S1). We integrated the dispersal kernel over observed variation in wind speeds, seed terminal velocity, and release height within the height of a shrub. Therefore the dispersal kernel for a shrub of height H was given by:

$$K_{disp} = \iiint p(F)p(U)p(z)p(r)\, dF\, dU\, dz \tag{4}$$

and $p(F)$ and $p(U)$ are the PDFs of the terminal velocity F and wind speed U, respectively, and $p(z)$ is the uniform distribution from the minimum seed release height (0.15m, the height at which grass cover interferes with wind dispersal) to H. Methods for our seed data collection and technical details of dispersal kernel modeling are provided in Appendix S1.

Spatial integral projection model

We used a spatial integral projection model to piece together seed dispersal and density-dependent demography, and generate predictions for the rate of shrub expansion that results from this combination of local and spatial processes. The spatially explicit model builds upon the non-spatial model (Eq. 1) and adds a spatial variable (z, z') such that demographic transitions occur across both time and space according to a combined demography-dispersal kernel $\tilde{K}$:

$$n(x', z', t+1) = \int_{-\infty}^{+\infty} \int_{x_{min}}^{x_{max}} \tilde{K}(x', x, z', z, \tilde{n}(z, t)) n(x, z, t)\, dx\, dz \tag{5}$$

Here, $\tilde{K}(x', x, z', z, \tilde{n}(z, t))$ describes the transition from size x and location z to size x' and location z' given density $\tilde{n}(z, t)$ at starting location z. As before, $\tilde{n}$ is a function of

19

population structure – in our model, weighted local density – but here integrated over an explicit competitive "neighborhood":

$$\tilde{n}(z,t) = \int_{z-h}^{z+h} \int_{x_{min}}^{x_{max}} x n(x,z,t) \, dx \, dz \tag{6}$$

where h represents neighborhood size in the units of z. The demography-dispersal kernel $\tilde{K}$ is given by the sum of two parts, one that describes reproduction coupled with dispersal of propagules, and another that describes growth and survival of non-dispersing individuals:

$$\tilde{K}(x',x,z',z,\tilde{n}(z,t)) = K_{disp}(z'-z)Q(x',x,\tilde{n}) + \delta(z'-z)G(x',x,\tilde{n}) \tag{7}$$

Here, the regeneration function Q and growth-survival function G correspond to Eq. 2, dispersal kernel K_{disp} corresponds to Eq. 7, and the Dirac delta function ($\delta(z'-z)$) is a probability distribution with all mass at zero, which prevents movement during survival and size transition. Following standard assumptions for integro-difference equations, we assume that space is one-dimensional and homogeneous, such that demographic transitions do not depend on location (or, more precisely, that they depend on location only through spatial variation in density) and the probability of dispersing from location z to $z\prime$ depends only on the absolute distance between them.

Under many conditions, models of this form generate traveling waves, and we are particularly interested in the velocity (m/yr) of this wave. Methods to estimate this velocity depend strongly on how demography responds to density. If fitness is maximized at some density $\tilde{n} > 0$ then the wave is pushed and wave velocity can only be estimated through numerical simulation. However, if fitness is maximized at $\tilde{n} = 0$ then the wave is pulled and an upper bound on its asymptotic velocity can be calculated analytically,

20

following Neubert and Caswell (2000) and Jongejans et al. (2011), as

$$c^* = \min_{s>0} \left[\frac{1}{s} \ln(\rho_s) \right] \tag{8}$$

where s is a wave shape parameter and ρ_s is the dominant eigenvalue of the kernel $H_s(x\prime, x)$. Corresponding to Eq. 7 and assuming $\tilde{n} = 0$, H_s is composed of

$$H_s(x\prime, x) = M(s, x)Q(x\prime, x) + G(x\prime, x) \tag{9}$$

where $M(s, x)$ is the moment-generating function (MGF) for the dispersal kernel associated with size x. This formulation of the model assumes that the dispersal kernel depends only on maternal size x and not offspring size $x\prime$. To estimate $M(s, x)$ we simulated $N = 10000$ dispersal events (r) for each size x and marginalized these over one spatial dimension as in Lewis et al. (2006). We then evaluated the empirical MGF for each size x: $M(s) = \frac{1}{N} \sum_{i=1}^{N} e^{sr}$.

We used numerical sensitivity analysis to compare the contributions of demography and dispersal processes to the speed of expansion. We perturbed each vital rate function by an arbitrary value, recalculated wavespeed, and quantified sensitivity as the change in wavespeed divided by the perturbation. Analytical sensitivity analysis is also possible (Ellner et al., 2016) but these sensitivities reflect infinitesmally small perturbations. We were particularly interested in the effects of large perturbations, especially large changes in seedling recruitment, which is subject to pulse events.

Estimates of wavespeed and its sensitivity to demography and dispersal processes were bootstrapped for a total of 1000 replicates. Each bootstrap replicate recreated size- and density-dependent demographic models using 50% resampling on the original demographic data, and recreated dispersal kernels also using 75% resampling on the wind

21

speeds and seed terminal velocities. Model selection for demographic vital rates was re-run for each bootstrap replicate. The empirical MGF relied on numerical sampling and was therefore sensitive to extreme long-distance events that differed across bootstrap realizations. Therefore, bootstrapped distributions reflect the combination of model uncertainty, parameter uncertainty, and stochasticity inherent to empirical MGFs.

Results

What are the strength and direction of density dependence in demographic vital rates along shrub encroachment ecotones?

Demographic data from naturally occurring and transplanted individuals revealed strong size- and density-dependence in demographic vital rates. For most sizes and vital rates, shrub density had negative demographic effects; there was no strong evidence for positive density dependence in any demographic process at any size. Statistical support for size- and density-dependence is provided in Appendix S2 (Tables S1–S6), which provide AIC rankings for candidate models based on the complete data set. In Figure 3, size is discretized into four groups evenly spaced from minimum to maximum size; this is for visualization purposes only.

Survival. Among naturally occurring plants, survival of large, established individuals was very high (Fig. 3A). We observed relatively few mortality events and nearly all of these were among new recruits. The probability of survival at these small sizes declined with increasing density. Survival of transplants was very low, lower even than survival of similarly-sized, naturally occurring recruits (Fig. 3A). However, the transplant results support the general pattern of negative density dependence in survival. Among the

22

20 survivors, 15 of them occurred in transect windows below the median of weighted shrub density. In Appendix S2, we show that transplant mortality was dominated by negative effects of shrub density at the 5-m window scale, even when effects of local grass and shrub cover were included as alternative or additional statistical covariates, which suggests that this is the appropriate spatial scale for modeling density dependence in this system.

Growth. Current size was strongly predictive of future size, as expected, and there was weak negative density dependence in mean future size conditioned on current size (Fig. 3B). However, there was a stronger signal of density dependence in the variance of future size (Fig. 3B, inset). Plants at low density exhibited greater variance in growth trajectories and this was especially true at the smallest sizes. Thus, large increases (and decreases) in the size of new recruits were most likely to occur under low-density conditions.

Flowering and fruit production. Flowering probability was strongly size-dependent and and very weakly sensitive to local density (Fig. 3C). However, fertility of flowering plants was strongly negative density dependent, with greatest flower and fruit production by the largest plants at the lowest densities, and vice versa (Fig. 3D).

Recruitment and recruit size. We observed 32 natural recruitment events along our transects during the study years and our estimated recruitment rate, given total expected seed production in each window preceding the recruitment year, was very low (2.47×10^{-6}, 3E). While most recruitment events occurred at low density, this is also where most seed production was concentrated (Fig. 3E), and low-density windows were over-represented relative to high density. For these reasons we were more likely to observe recruiment events at low density. Controlling for sampling effort and seed production, the

23

statistical models indicated that our data were most consistent with a constant, density-independent seed-to-seedling recruitment rate (Table S6). However, the mean size of new recruits declined significantly with local density (Fig. 3F).

Population growth rate. As expected given the vital rate results, the asymptotic population growth rate λ declined monotonically with density (Fig. 4). This was true across $> 98\%$ of bootstrap replicates, indicating high certainty that shrub fitness is maximized at zero density and thus that the expansion wave is "pulled" (for this reason our wavespeed results are based on the analytical approach described above). Mean growth rate at low density was *ca.* 3% per year, with bootstrap uncertainty spanning 1–6%. At high density in the core of the expansion wave, population growth rates approached $\lambda = 1$, indicating population stasis driven by near-immortality and extremely rare recruitment.

What is the seed dispersal kernel and how does it vary with maternal plant size?

WALD dispersal kernels were modeled using the properties of seeds and wind and accounted for observed variation in wind speed, seed terminal velocity, and within-plant seed release height. The resulting kernels were predicted to be strongly size dependent, with taller plants having a greater probability of dispersing seeds longer distances (Fig. 5). However, predicted seed dispersal was highly local, with most seeds expected to fall within one meter of parent plants for most sizes. Even for the very tallest shrub we observed (1.96 m), only 6.2% of its seeds were predicted to fall more than 3 m away and less than 1% were predicted to fall more than 6 m away (Fig. 5). Taller shrubs also exhibited wider variance in their dispersal kernel, reflecting their wider range of within-shrub seed release heights.

24

What is the predicted rate of expansion and which lower-level processes most strongly affect the expansion speed?

The asymptotic speed of creosotebush encroachment, given the above demography and dispersal patterns, was very slow. The mean asymptotic speed was 0.08 m/year and the 5th–95th percentiles of the uncertainty distribution was 0.06–0.12 m/year (Fig. 6A). The sensitivities of wavespeed spanned orders of magnitude, indicating strong inequality in the relative importance of the demography and dispersal processes controlling expansion (Fig. 6B). Expansion speed was by far the most sensitive to the probability of seedling recruitment (Fig. 6B), indicating that this life cycle transition imposes the strongest constraint on encroachment. Sensitivity to survival ranked second, and since nearly all mortality occurred at the smallest sizes this too can be interpreted as an early life cycle constraint on expansion. The mean of growth ranked third and this was also likely related to early plant survival, since increases in size allow small plants to reach "protected" sizes given the strong size-dependence in survival.

Discussion

The encroachment of grasslands by woody plants is a worldwide phenomenon with broad implications for biodiversity and ecosystem function. A theoretical perspective rooted in spatial population biology brings attention to the combined influence of dispersal and density-dependent demography as critical controls on the occurrence and pace of encroachment. Through this lens, we hypothesized that recent stasis at the grass-shrub ecotone (Fig. 2) is driven by positive feedbacks that cause declines in fitness at the low-density front. Instead, observational and experimental evidence indicate that fitness was maximized in low-density plant neighborhoods. The creosotebush encroach-

25

ment wave is therefore predicted to be pulled by maximum demographic performance at the leading edge. However, our field-parameterized spatial integral projection model revealed that this wave is pulled at the very slow rate of 6–12 centimeters per year – so slow that this grass-shrub ecotone is predicted to be effectively stationary, consistent with observations. In fact, to our knowledge, this is the slowest plant population wavespeed estimated using SIPMs or their matrix model progenitors (Neubert and Caswell, 2000). Below, we discuss and interpret these key findings and their broader implications in greater detail.

Observational and experimental evidence strongly indicated that effects of shrub density were strongly negative in all vital rates and at all sizes. This was surprising given widespread evidence for positive feedbacks (which should generate low-density fitness penalties; i.e., Allee effects) in woody plant encroachment generally (D'odorico et al., 2013) and specifically in our creosotebush system (D'Odorico et al., 2010). How can we square these apparently conflicting results? First, it may be important to consider the distinction between "demographic" and "component" Allee effects (Stephens et al., 1999), which refer to effects that manifest in total fitness and components of fitness, respectively. That is, positive effects of conspecific density may occur, but in our measures of demographic performance these are swamped by stronger, counter-acting negative effects. It is worth noting that our demographic measurements are temporally coarse, reflecting aggregate performance over a full transition year. More mechanistic studies on finer time scales might reveal component Allee effects that are masked by strong net-negative density dependence. Second, many of the potential mechanisms for positive feedbacks at shrub-grass ecotones would manifest infrequently. For example, effects of shrub encroachment on microclimate (D'odorico et al., 2013) may promote shrub survival only in the face of rare climate events such as extreme low temperatures. Similarly,

26

positive feedbacks that occur via fire suppression (Collins et al., 2021; Ratajczak et al., 2011) would only manifest on timescales that are inclusive of fire return intervals. These considerations suggest that we may be more likely to detect positive density dependence over longer time scales encompassing conditions that trigger positive feedbacks. This leads to the hypothesis that the shrub encroachment wave is *usually* pulled but occasionally pushed. To our knowledge such switches have never been empirically documented in any expanding population but may be an important feature of expansion in fluctuating environments.

The very low transplant survival and recruitment rates that we measured also call attention to time scale. Previous studies suggest that creosotebush recruitment is strongly episodic, likely in response to large, infrequent monsoon precipitation events (Allen et al., 2008; Boyd and Brum, 1983; Moreno-de las Heras et al., 2016). Similar patterns of episodic recruitment driven by large precipitation events have been observed in other cases of woody plant encroachment in aridlands (Harrington, 1991; Weber-Grullon et al., 2022), and relatively high transplant survival on the one transect that we planted immediately following a large monsoon event anecdotally supports an important role for pulses of soil moisture. With only four transition-years of demographic data, we chose to combine information across years and build a deterministic model that averages over inter-annual variability. However, the connection between shrub recruitment and monsoon precipitation, combined with the observed and projected increase in the variability of monsoon precipitation in our study region (Petrie et al., 2014; Rudgers et al., 2018), suggest that extending our deterministic model to accommodate inter-annual variability in climate and climate-dependent vital rates will be a critical next step. Because our wavespeed estimate is acutely sensitive to the seed-to-seedling transition, much more so than any other demographic or dispersal process, we expect that a stochastic model incorporating many

27

years of data may yield a faster predicted expansion speed driven by rare pulses of re-cruitment (Ellner and Schreiber, 2012). Such pulses have clearly not occurred during our study years (2013–2017) or the preceding decade of transect re-surveys (2001–2012) and therefore we think the deterministic model is an adequate representation of recent condi-tions. However, our findings of pulled-wave dynamics and strong wavespeed sensitivity to seedling recruitment indicate that the present shrub ecotone is primed for expansion once the necessary climate conditions align, as they likely will in a more variable cli-mate regime. While monsoon precipitation is a leading candidate for factors promoting seedling establishment, it is worth noting that our study years included both the lowest and second-highest amounts of monsoon precipitation in a 20-year record, and yet these events did not correlate with seedling recruitment on our transects (Appendix S2, Fig. S1). The conditions favoring recruitment and recruit survival may therefore be more complicated than the single driver of monsoon precipitation.

While not as strong a constraint based on our sensitivity analysis, limited dispersal ability also contributed to the very slow predicted speed of encroachment. Our findings of very limited dispersal are consistent with a previous study that found creosotebush seeds in the seed bank were found only beneath mature shrubs and not in nearby grass patches or inter-plant spaces (Moreno-de las Heras et al., 2016). Our mechanistic dis-persal modeling assumes that wind is the sole dispersal vector. Previous work suggests that this modeling approach can accurately predict dispersal patterns for wind-dispersed plants (Skarpaas and Shea, 2007), yet in our system it may be important to consider sec-ondary dispersal vectors. Boyd and Brum's 1983 study of creosotebush reproductive biology described "contradiction in the literature about mode of dispersal", citing evi-dence for a dominant role of wind but the additional possibility of seed movement by granivorous animals. Combining wind and animal dispersal vectors into a "total" dis-

persal kernel (Rogers et al., 2019) will be a valuable next step. Second, overland flow of runoff may contribute to secondary seed movement following initial deposition by wind (Thompson et al., 2014). Interestingly, seed movement from overland flow would be most likely following large monsoon events. Therefore, the same conditions that promote seedling recruitment may also promote long-distance dispersal, potentially amplifying a pulse of shrub encroachment (Ellner and Schreiber, 2012). Seeds may also be blown along the ground following initial deposition, which our model does not account for. The classic WALD dispersal model employed here assumes uniform grass cover, with seeds trapped below the height of this grass canopy. As in aridlands worldwide, our nothern Chihuahuan Desert study region is characterized by a high percentage of bare ground, especially in areas of high creosotebush density (Fig. 1). New approaches are needed to extend mechanistic dispersal modeling to accommodate this feature of aridlands, as others have recognized (Thompson et al., 2014). The potential roles for both biotic and abiotic secondary dispersal vectors makes our dispersal kernel a conservative estimate of seed movement and highlights a need for further study of shrub seed dispersal.

Our model focused on intra-specific density dependence but inter-specific plant-plant interactions may be an important element of shrub encroachment, or lack thereof. For example, over-grazing is a hypothesized driver of shrub encroachment due to release from grass competition and reduction of grassland fires (Van Auken, 2000). Our shrub encroachment model considered only one "side" of the grass-shrub ecotone, assuming that the shrub population spreads into empty space. Explicit consideration of grass competition or facilitation may enrich our understanding of shrub advance or stasis in this and other systems (Sankaran et al., 2004). However, our transplant experiment suggested weak negative effects of grass cover on seedling survival (Appendix S3, Fig.

S1B). Similarly, grass competition had no effect on germination and survival of mesquite (*Prosopis glandulosa*) shrubs in Chihuahuan Desert grassland (Weber-Grullon et al., 2022). While our current data do not allow us to quantify whether and how strongly resident grasses may slow down shrub encroachment, we can infer that competitive effects of grasses on shrubs are weaker than competitive effects of shrubs on shrubs. Therefore our conclusion that the encroachment wave is pulled implicitly accounts for any effects of grass cover.

While our data reveal strong negative density dependence, we know little about the underlying mechanisms that give rise to this pattern. What is it about high shrub density environments that suppress survival and reproduction? The abundance of bare ground in core shrubland suggests that shrubs do not compete for space. However, Brisson and Reynolds (1994) found strong competition for space belowground, with crowded neighborhoods constraining creosotebush root systems. Also, root development of creosotebush seedlings can respond rapidly to the availability of soil moisture (Obrist and Arnone III, 2003), suggesting that competition for water may be another element of density dependence. Finally, negative density dependence in plants may also be mediated by consumers or soil microbes. Better understanding the environmental drivers of density dependence will enable better prediction for how the encroachment wave may respond to future environmental change.

Our model was parameterized specifically for the creosotebush system, but the body of theory upon which it is based is broadly applicable to other woody encroachment systems. Examples from the literature provide interesting points of similarity and contrast. Encroaching *Acacia mellifera* in Namibian savanna experience negative density dependence in seedling survival (Joubert et al., 2013), and leading-edge colonists at boreal treelines experience a growth advantage over established trees (Dial et al., 2022); both are

30

consistent with pulled-wave encroachment dynamics, as we observed in creosotebush. On the other hand, *Acacia drepanolobium* in East African savanna experiences positive feedbacks that arise from mutualism with defensive ants (higher-density tree aggregations support larger populations of defenders), which promotes the stability of monodominant stands but generate pushed-wave dynamics that limit encroachment (Kenfack et al., 2021). In another pushed-wave example, woody plants in Brazilian Cerrado facilitate both the arrival and establishment of other woody species by attracting seed-dispersing birds and amelioratng stressful soil conditions (Abreu et al., 2021). Clearly, the pace and underlying mechanisms of encroachment may exhibit wide variation across species or systems depending on the nature of density-dependent feedbacks as well as external drivers such as fire suppression, grazing, and climate change. The general demography-dispersal framework developed here may provide a unifying lens to understand and predict woody encroachment in diverse systems, from arctic treeline to aridland savanna to salt marsh ecosystems (Kelleway et al., 2017). Furthermore, trait-based approaches may help explain variation in encroachment speed across species or systems and identify which are prone to pushed or pulled dynamics. For example, in two of the examples above, reliance on animal mutualists for defense or dispersal generated positive density-dependent feedbacks.

Conclusions. Understanding and predicting the dynamics of woody-herbaceous ecotones requires that we build knowledge of the fates of the rare individuals that disperse from core habitat and cross habitat boundaries. For a creosotebush, there is no better place to be than alone in a grassland, and that key result governs the spatial dynamics of this population. We found that the wave of creosotebush expansion into Chihuahuan desert grassland is pulled by peak fitness at the leading edge. However, it is pulled so slowly that it is effectively stalled, a model-derived prediction that recapitulates obser-

31

vations on the ground. Had we only relied on the re-survey data without insight from the mechanistic model we might have concluded that the creosotebush ecotone is stable at its current boundary. Instead, acute sensitivity of a slow wave to seedling recruitment leaves this system poised for pulses of expansion under the right conditions; what exactly those conditions are is not yet fully resolved. We suggest that the concepts and tools of spatial population biology may facilitate advances in the study and management of woody plant encroachment, which, like all spreading populations, must be driven by birth, death, and movement.

Acknowledgements

Author contributions

All authors contributed to study design. THD and TEXM led data analysis, modeling, and writing early drafts of the manuscript. All authors participated in preparing the manuscript for submission.

Literature Cited

Abreu, R. C., G. Durigan, A. C. Melo, N. A. Pilon, and W. A. Hoffmann. 2021. Facilitation by isolated trees triggers woody encroachment and a biome shift at the savanna–forest transition. Journal of Applied Ecology **58**:2650–2660.

Allen, A., W. Pockman, C. Restrepo, and B. Milne. 2008. Allometry, growth and population regulation of the desert shrub Larrea tridentata. Functional Ecology pages 197–204.

Bowers, J. E., R. M. Turner, and T. L. Burgess. 2004. Temporal and spatial patterns in emergence and early survival of perennial plants in the Sonoran Desert. Plant Ecology **172**:107–119.

Boyd, R. S., and G. D. Brum. 1983. Postdispersal reproductive biology of a Mojave Desert population of Larrea tridentata (Zygophyllaceae). American Midland Naturalist pages 25–36.

Brandt, J. S., M. A. Haynes, T. Kuemmerle, D. M. Waller, and V. C. Radeloff. 2013. Regime shift on the roof of the world: Alpine meadows converting to shrublands in the southern Himalayas. Biological Conservation **158**:116–127.

Brisson, J., and J. F. Reynolds. 1994. The effect of neighbors on root distribution in a creosotebush (Larrea tridentata) population. Ecology **75**:1693–1702.

Buffington, L. C., and C. H. Herbel. 1965. Vegetational changes on a semidesert grassland range from 1858 to 1963. Ecological monographs **35**:139–164.

Cabral, A., J. De Miguel, A. Rescia, M. Schmitz, and F. Pineda. 2003. Shrub encroachment in Argentinean savannas. Journal of Vegetation Science **14**:145–152.

33

Collins, S. L., J. B. Nippert, J. M. Blair, J. M. Briggs, P. Blackmore, and Z. Ratajczak. 2021. Fire frequency, state change and hysteresis in tallgrass prairie. Ecology Letters **24**:636–647.

Dial, R. J., C. T. Maher, R. E. Hewitt, and P. F. Sullivan. 2022. Sufficient conditions for rapid range expansion of a boreal conifer. Nature **608**:546–551.

D'Odorico, P., J. D. Fuentes, W. T. Pockman, S. L. Collins, Y. He, J. S. Medeiros, S. DeWekker, and M. E. Litvak. 2010. Positive feedback between microclimate and shrub encroachment in the northern Chihuahan desert. Ecosphere **1**:1–11.

D'odorico, P., Y. He, S. Collins, S. F. De Wekker, V. Engel, and J. D. Fuentes. 2013. Vegetation–microclimate feedbacks in woodland–grassland ecotones. Global Ecology and Biogeography **22**:364–379.

D'Odorico, P., G. S. Okin, and B. T. Bestelmeyer. 2012. A synthetic review of feedbacks and drivers of shrub encroachment in arid grasslands. Ecohydrology **5**:520–530.

Duran, K. L., T. K. Lowrey, R. R. Parmenter, and P. O. Lewis. 2005. Genetic diversity in Chihuahuan Desert populations of creosotebush (Zygophyllaceae: Larrea tridentata). American Journal of Botany **92**:722–729.

Ellner, S. P., D. Z. Childs, M. Rees, et al. 2016. Data-driven modelling of structured populations. A practical guide to the Integral Projection Model. Cham: Springer .

Ellner, S. P., and S. J. Schreiber. 2012. Temporally variable dispersal and demography can accelerate the spread of invading species. Theoretical Population Biology **82**:283–298.

Gandhi, S. R., E. A. Yurtsev, K. S. Korolev, and J. Gore. 2016. Range expansions transition from pulled to pushed waves as growth becomes more cooperative in an experimental microbial population. Proceedings of the National Academy of Sciences **113**:6922–6927.

Gardner, J. L. 1951. Vegetation of the creosotebush area of the Rio Grande Valley in New Mexico. Ecological Monographs **21**:379–403.

Gibbens, R., R. McNeely, K. Havstad, R. Beck, and B. Nolen. 2005. Vegetation changes in the Jornada Basin from 1858 to 1998. Journal of Arid Environments **61**:651–668.

Goslee, S., K. Havstad, D. Peters, A. Rango, and W. Schlesinger. 2003. High-resolution images reveal rate and pattern of shrub encroachment over six decades in New Mexico, USA. Journal of Arid Environments **54**:755–767.

Grover, H. D., and H. B. Musick. 1990. Shrubland encroachment in southern New Mexico, USA: an analysis of desertification processes in the American Southwest. Climatic change **17**:305–330.

Harrington, G. N. 1991. Effects of soil moisture on shrub seedling survival in semi-arid grassland. Ecology **72**:1138–1149.

Huang, H., L. D. Anderegg, T. E. Dawson, S. Mote, and P. D'Odorico. 2020. Critical transition to woody plant dominance through microclimate feedbacks in North American coastal ecosystems. Ecology **101**:e03107.

Jongejans, E., K. Shea, O. Skarpaas, D. Kelly, and S. P. Ellner. 2011. Importance of individual and environmental variation for invasive species spread: a spatial integral projection model. Ecology **92**:86–97.

Joubert, D. F., G. Smit, and M. T. Hoffman. 2013. The influence of rainfall, competition and predation on seed production, germination and establishment of an encroaching Acacia in an arid Namibian savanna. Journal of Arid Environments **91**:7–13.

Katul, G., A. Porporato, R. Nathan, M. Siqueira, M. Soons, D. Poggi, H. Horn, and S. A.

35

Levin. 2005. Mechanistic analytical models for long-distance seed dispersal by wind. The American Naturalist **166**:368–381.

Keitt, T. H., M. A. Lewis, and R. D. Holt. 2001. Allee effects, invasion pinning, and species' borders. The American Naturalist **157**:203–216.

Kelleway, J. J., K. Cavanaugh, K. Rogers, I. C. Feller, E. Ens, C. Doughty, and N. Saintilan. 2017. Review of the ecosystem service implications of mangrove encroachment into salt marshes. Global Change Biology **23**:3967–3983.

Kenfack, D., G. Arellano, S. Kibet, D. Kimuyu, and P. Musili. 2021. Understanding the monodominance of Acacia drepanolobium in East African savannas: insights from demographic data. Trees **35**:1439–1450.

Knapp, A. K., J. M. Briggs, S. L. Collins, S. R. Archer, M. S. BRET-HARTE, B. E. Ewers, D. P. Peters, D. R. Young, G. R. Shaver, E. Pendall, et al. 2008. Shrub encroachment in North American grasslands: shifts in growth form dominance rapidly alters control of ecosystem carbon inputs. Global Change Biology **14**:615–623.

Kot, M., M. A. Lewis, and P. van den Driessche. 1996. Dispersal data and the spread of invading organisms. Ecology **77**:2027–2042.

Lewis, M., and P. Kareiva. 1993. Allee dynamics and the spread of invading organisms. Theoretical Population Biology **43**:141–158.

Lewis, M. A., M. G. Neubert, H. Caswell, J. S. Clark, and K. Shea, 2006. A guide to calculating discrete-time invasion rates from data. Pages 169–192 *in* Conceptual ecology and invasion biology: reciprocal approaches to nature. Springer.

Mabry, T. J., J. H. Hunziker, D. Difeo Jr, et al. 1978. Creosote bush: biology and chemistry of Larrea in New World deserts. Dowden, Hutchinson & Ross, Inc.

36

Maddox, J. C., and S. Carlquist. 1985. Wind dispersal in Californian desert plants: experimental studies and conceptual considerations. Aliso: A Journal of Systematic and Evolutionary Botany **11**:77–96.

McAuliffe, J., E. Hamerlynck, and M. Eppes. 2007. Landscape dynamics fostering the development and persistence of long-lived creosotebush (Larrea tridentata) clones in the Mojave Desert. Journal of Arid Environments **69**:96–126.

Moore, D., and K. Hall, 2022. Meteorology Data from the Sevilleta National Wildlife Refuge, New Mexico. Environmental Data Initiative. https://doi.org/10.6073/pasta/d56307b398e28137dabaa6994f0f5f92.

Moreno-de las Heras, M., L. Turnbull, and J. Wainwright. 2016. Seed-bank structure and plant-recruitment conditions regulate the dynamics of a grassland-shrubland Chihuahuan ecotone. Ecology **97**:2303–2318.

Morford, S. L., B. W. Allred, D. Twidwell, M. O. Jones, J. D. Maestas, C. P. Roberts, and D. E. Naugle. 2022. Herbaceous production lost to tree encroachment in United States rangelands. Journal of Applied Ecology **59**:2971–2982.

Nathan, R., G. G. Katul, G. Bohrer, A. Kuparinen, M. B. Soons, S. E. Thompson, A. Trakhtenbrot, and H. S. Horn. 2011. Mechanistic models of seed dispersal by wind. Theoretical Ecology **4**:113–132.

Neubert, M. G., and H. Caswell. 2000. Demography and dispersal: calculation and sensitivity analysis of invasion speed for structured populations. Ecology **81**:1613–1628.

Obrist, D., and J. Arnone III. 2003. Increasing CO_2 accelerates root growth and enhances

water acquisition during early stages of development in Larrea tridentata. New Phytologist **159**:175–184.

Pan, S., and G. Lin. 2012. Invasion traveling wave solutions of a competitive system with dispersal. Boundary Value Problems **2012**:120.

Parizek, B., C. M. Rostagno, and R. Sottini. 2002. Soil erosion as affected by shrub encroachment in northeastern Patagonia. Rangeland Ecology & Management/Journal of Range Management Archives **55**:43–48.

Peters, D. P., and J. Yao. 2012. Long-term experimental loss of foundation species: consequences for dynamics at ecotones across heterogeneous landscapes. Ecosphere **3**:1–23.

Petrie, M., S. Collins, D. Gutzler, and D. Moore. 2014. Regional trends and local variability in monsoon precipitation in the northern Chihuahuan Desert, USA. Journal of Arid Environments **103**:63–70.

Ratajczak, Z., J. B. Nippert, and S. L. Collins. 2012. Woody encroachment decreases diversity across North American grasslands and savannas. Ecology **93**:697–703.

Ratajczak, Z., J. B. Nippert, J. C. Hartman, and T. W. Ocheltree. 2011. Positive feedbacks amplify rates of woody encroachment in mesic tallgrass prairie. Ecosphere **2**:1–14.

Ravi, S., P. D'Odorico, S. L. Collins, and T. E. Huxman. 2009. Can biological invasions induce desertification? The New Phytologist **181**:512–515.

Reed, M., L. Stringer, A. Dougill, J. Perkins, J. Atlhopheng, K. Mulale, and N. Favretto. 2015. Reorienting land degradation towards sustainable land management: Linking sustainable livelihoods with ecosystem services in rangeland systems. Journal of environmental management **151**:472–485.

Reynolds, J. F., R. A. Virginia, P. R. Kemp, A. G. De Soyza, and D. C. Tremmel. 1999. Impact of drought on desert shrubs: effects of seasonality and degree of resource island development. Ecological Monographs **69**:69–106.

Rogers, H. S., N. G. Beckman, F. Hartig, J. S. Johnson, G. Pufal, K. Shea, D. Zurell, J. M. Bullock, R. S. Cantrell, B. Loiselle, et al. 2019. The total dispersal kernel: a review and future directions. AoB Plants **11**:plz042.

Roques, K., T. O'connor, and A. R. Watkinson. 2001. Dynamics of shrub encroachment in an African savanna: relative influences of fire, herbivory, rainfall and density dependence. Journal of Applied Ecology **38**:268–280.

Rudgers, J. A., Y. A. Chung, G. E. Maurer, D. I. Moore, E. H. Muldavin, M. E. Litvak, and S. L. Collins. 2018. Climate sensitivity functions and net primary production: a framework for incorporating climate mean and variability. Ecology **99**:576–582.

Sankaran, M., J. Ratnam, and N. P. Hanan. 2004. Tree–grass coexistence in savannas revisited–insights from an examination of assumptions and mechanisms invoked in existing models. Ecology letters **7**:480–490.

Schlesinger, W. H., and A. M. Pilmanis. 1998. Plant-soil interactions in deserts. Biogeochemistry **42**:169–187.

Schlesinger, W. H., J. A. Raikes, A. E. Hartley, and A. F. Cross. 1996. On the spatial pattern of soil nutrients in desert ecosystems: ecological archives E077-002. Ecology **77**:364–374.

Schlesinger, W. H., J. F. Reynolds, G. L. Cunningham, L. F. Huenneke, W. M. Jarrell, R. A. Virginia, and W. G. Whitford. 1990. Biological feedbacks in global desertification. Science **247**:1043–1048.

Sirami, C., and A. Monadjem. 2012. Changes in bird communities in Swaziland savannas between 1998 and 2008 owing to shrub encroachment. Diversity and Distributions **18**:390–400.

Skarpaas, O., and K. Shea. 2007. Dispersal patterns, dispersal mechanisms, and invasion wave speeds for invasive thistles. The American Naturalist **170**:421–430.

Stephens, P. A., W. J. Sutherland, and R. P. Freckleton. 1999. What is the Allee effect? Oikos pages 185–190.

Sullivan, L. L., B. Li, T. E. Miller, M. G. Neubert, and A. K. Shaw. 2017. Density dependence in demography and dispersal generates fluctuating invasion speeds. Proceedings of the National Academy of Sciences **114**:5053–5058.

Taylor, C. M., and A. Hastings. 2005. Allee effects in biological invasions. Ecology Letters **8**:895–908.

Thompson, S. E., S. Assouline, L. Chen, A. Trahktenbrot, T. Svoray, and G. G. Katul. 2014. Secondary dispersal driven by overland flow in drylands: Review and mechanistic model development. Movement ecology **2**:7.

Trollope, W., F. Hobson, J. Danckwerts, and J. Van Niekerk. 1989. Encroachment and control of undesirable plants. Veld management in the Eastern Cape pages 73–89.

Turnbull, L., J. Wainwright, and R. E. Brazier. 2010. Changes in hydrology and erosion over a transition from grassland to shrubland. Hydrological Processes: An International Journal **24**:393–414.

Van Auken, O. 2009. Causes and consequences of woody plant encroachment into western North American grasslands. Journal of environmental management **90**:2931–2942.

Van Auken, O. W. 2000. Shrub invasions of North American semiarid grasslands. Annual review of ecology and systematics **31**:197–215.

Vasek, F. C. 1980. Creosote bush: Long-lived clones in the Mojave Desert. American Journal of Botany **67**:246–255.

Veit, R. R., and M. A. Lewis. 1996. Dispersal, population growth, and the Allee effect: dynamics of the house finch invasion of eastern North America. The American Naturalist **148**:255–274.

Wang, M.-H., M. Kot, and M. G. Neubert. 2002. Integrodifference equations, Allee effects, and invasions. Journal of mathematical biology **44**:150–168.

Weber-Grullon, L., L. Gherardi, W. A. Rutherford, S. R. Archer, and O. E. Sala. 2022. Woody-plant encroachment: Precipitation, herbivory, and grass-competition interact to affect shrub recruitment. Ecological Applications **32**:e2536.

Wilcox, B. P., A. Birt, S. D. Fuhlendorf, and S. R. Archer. 2018. Emerging frameworks for understanding and mitigating woody plant encroachment in grassy biomes. Current Opinion in Environmental Sustainability **32**:46–52.

Williams, J. L., T. E. Miller, and S. P. Ellner. 2012. Avoiding unintentional eviction from integral projection models. Ecology **93**:2008–2014.

Wood, S. 2017. Generalized Additive Models: An Introduction with R. 2 edition. Chapman and Hall/CRC.

Figure legends

Figure 1. Example of an ecotone transect spanning gradients of creosotebush and black grama grass at Sevilleta National Wildlife Refuge, a Long-Term Ecological Research (LTER) site in central New Mexico, US.

Figure 2. Surveys of creosotebush percent cover along two permanent transects (A,B) in 2001 and 2013. In summer 2001, shrub percent cover was recorded along two permanent 1000-m transects that spanned the shrub-grass ecotone. Surveys were conduced again in summer 2013. At every 10 meters, shrub cover was recorded in nine cover classes (<1%, 1–4%, 5–10%, 10–25%, 25–33%, 33–50%, 50–75%, 75–95%, >95%). This figure shows mid-point values of these cover classes at each meter location for both transects and years.

Figure 3. Size- and density-dependence in demographic vital rates. **A** Probability of survival from natural population census and transplant experiment (black line), **B** Mean and variance (inset) of size conditional on previous size, **C** Probability of flowering, **D** Flower and fruit production, **E** Probability of recruitment per seed, **F** Recruit size. In **A**–**D**, colored lines indicate four size groups (red is largest, blue is smallest), discretized for data visualization only. In all panels, weighted density is the sum of all plant sizes $log(cm^3)$ within the same 5-m window as the census individual. In panels **A** and **C**, points indicate binned means and point size is proportional to sample size for the mean.

Figure 4. Density dependence in the asymptotic population growth rate (λ). Gray lines show bootstrap replicates and the black lines shows predictions from full demographic data set. Weighted deighted density is the sum of all plant sizes $log(cm^3)$ within 5-m windows.

Figure 5. Predicted WALD dispersal kernels for four shrub heights corresponding to the 25th, 50th, 75th, and 100th (maximum) percentiles of the observed size distribution. We

42

assume that heights below 15 cm have effectively no seed movement due to interference with the grass layer.

Figure 6. A, Asymptotic speed of creosotebush encroachment. The distribution reflects parameter and model uncertainties quantified via bootstrapping and stochastic sampling from seed dispersal kernels. B, Sensitivities of wavespeed to demography and dispersal processes. For size-dependent functions (growth, survival, flowering, and fertility) sensitivity was calculate by perturbing the entire function across all sizes.
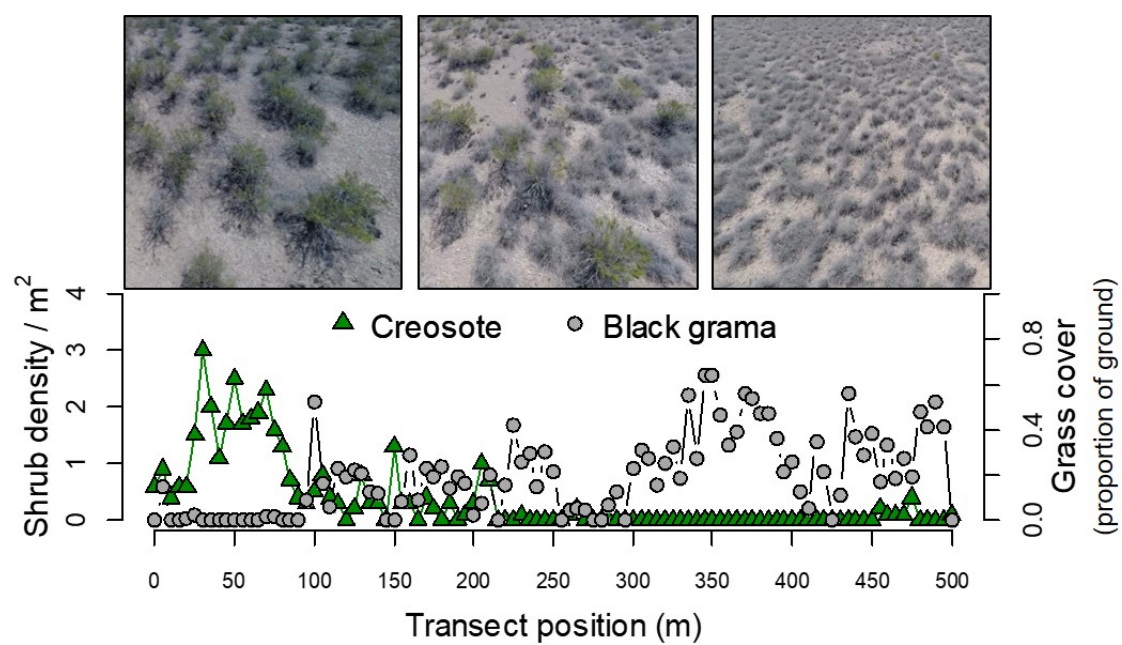
Figure 1
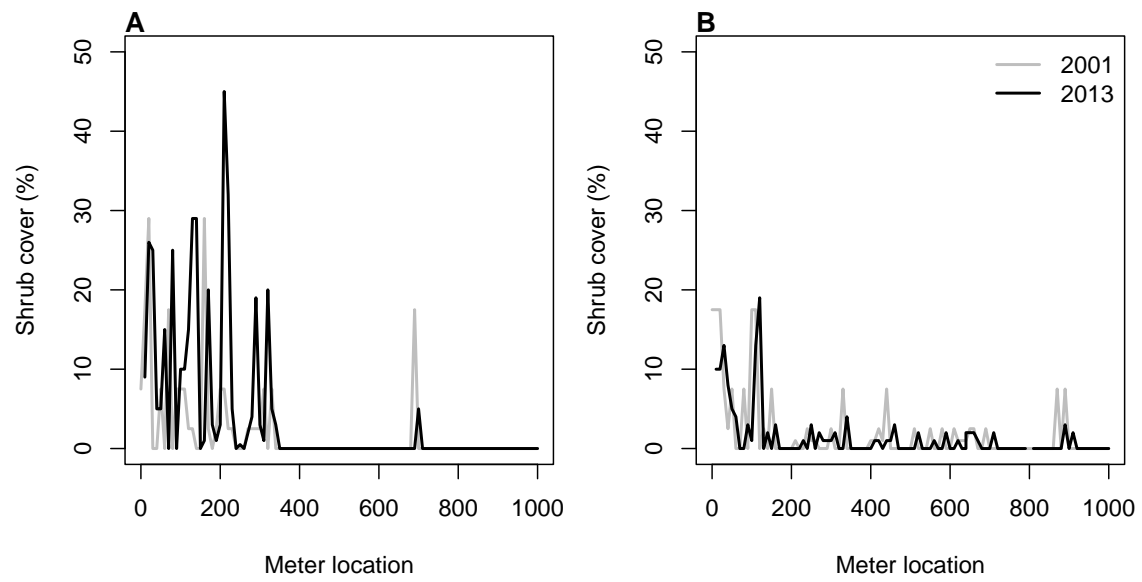
Figure 2
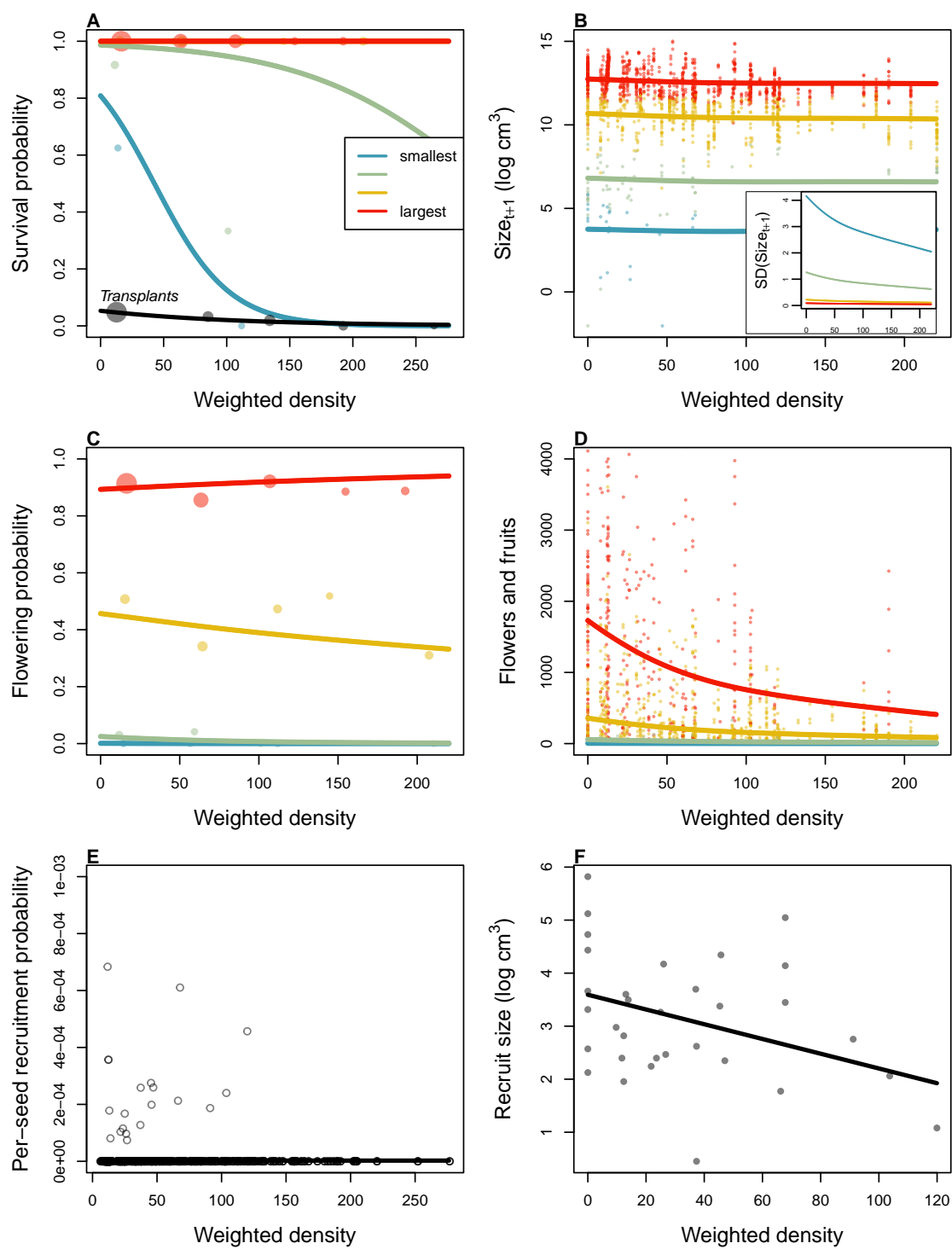
Figure 3
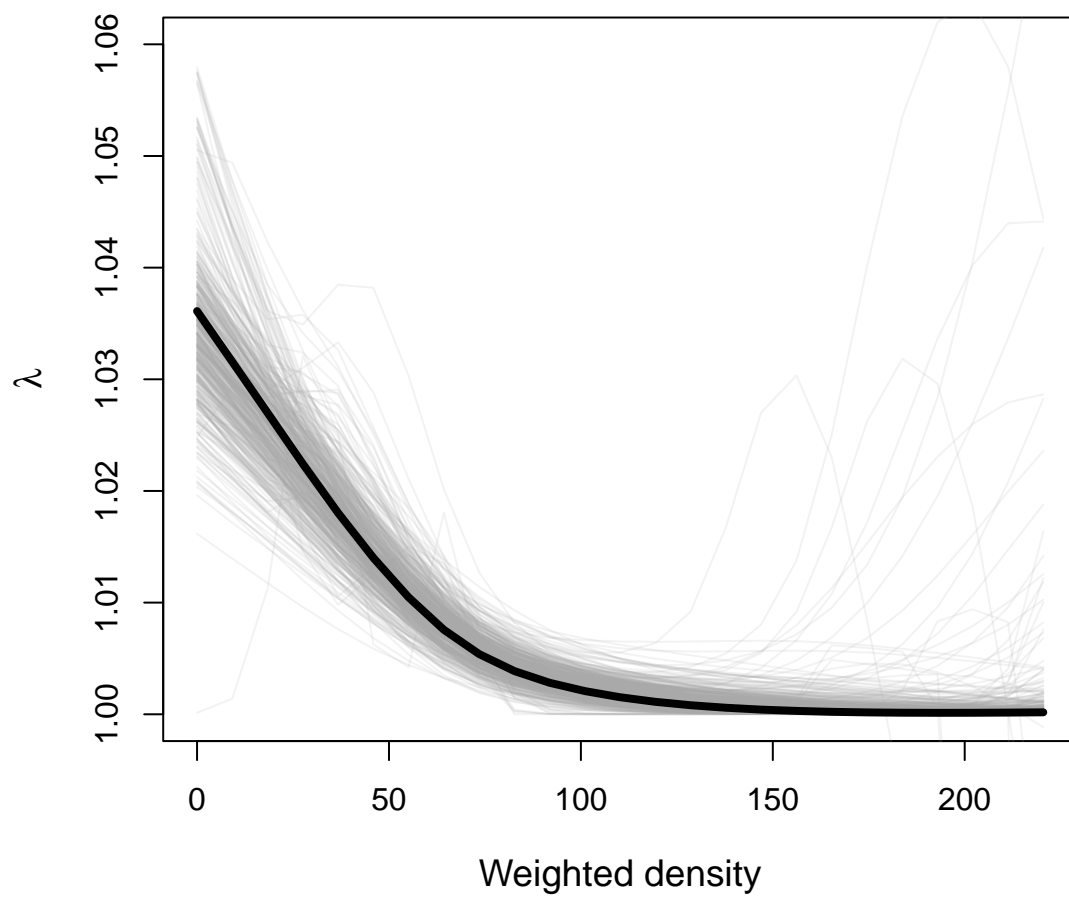
Figure 4

Figure 5

Figure 6